

Self-consistent low-energy meson mass spectrum

Louis A. P. Balázs

Physics Department, Purdue University, West Lafayette, Indiana 47907

(Received 13 February 1979)

In a typical hadron mass calculation the long-range (confining) part of the interaction between quarks (q) is assumed to be spin-independent. Any spin dependence is then attributed to short-range one-gluon exchange. This procedure tends to give an excessively small mass difference between pseudoscalar (P) and vector (V) mesons, at least if the quark-gluon coupling is fixed by other properties of the hadron spectrum. In the present paper we introduce an approach in which a large P - V mass difference arises naturally. A confining interaction does not have to be assumed *a priori*. The spectrum is generated by imposing duality on an infinite sum of ladder graphs without crossed quark lines; this "planar bootstrap" corresponds to the limit $N_{\text{flavor}} \rightarrow \infty$ (in quantum chromodynamics we would have to take $N_{\text{color}} \rightarrow \infty$ at the same time). By making a certain simple dynamical approximation we then derive an explicit infinitely rising exchange-degenerate leading Regge trajectory $\alpha(t) = S_1 + S_2 + \mathcal{L}(v_a)$ for any given equal-mass-channel hadron + hadron \rightarrow hadron + hadron process; S_1 and S_2 are external spins, $\mathcal{L}(v_a) \simeq -0.5 + 2\alpha'v_a$, and $v_a = s_a + (t - \Sigma m_i^2)/2$, where the m_i are the external masses and $\sqrt{s_a}$ is the mass of an exchanged cluster a . By requiring the s_a to be as low as possible and imposing simultaneous consistency for complete sets of meson + meson \rightarrow meson + meson processes, we are able to calculate the entire natural- and unnatural-parity low-energy leading-trajectory $q\bar{q}$ mass spectrum in terms of m_ρ and m_{K^*} alone. We obtain $m_\pi^2 \ll m_\rho^2$, a universal Regge slope $\alpha' = (m_\rho^2 - m_\pi^2)^{-1}/2$, and the usual mass formulas $m_\phi^2 - m_{K^*}^2 = m_{K^*}^2 - m_\rho^2 = m_K^2 - m_\pi^2 = m_{\eta_8}^2 - m_K^2$, $m_\omega = m_\rho$. In the case of $\eta_u = (u\bar{u} + d\bar{d})/\sqrt{2}$, however, we obtain $m_{\eta_u}^2 = 1/3(m_\rho^2 + 2m_\pi^2)$, which gives $m_{\eta_u} = 0.462$ GeV.

I. INTRODUCTION

In a quark-gluon field theory, such as quantum chromodynamics (QCD), the hadrons are treated as bound states of quarks (q). The short-range part of the interquark interaction is given by one-gluon exchange. The long-range part has not, as yet, been reliably calculated from the basic QCD Lagrangian, but is believed to be dominated by infrared singularities which lead to quark confinement. In practice, phenomenological potentials or bag boundary conditions are therefore simply assumed *a priori*. These are usually taken to be spin-independent, which by itself would lead to pseudoscalar-vector mass degeneracy. The breaking of this degeneracy is assumed to arise entirely from the short-range color-magnetic spin-spin part of one-gluon exchange.¹

Calculations based on the above picture have generally been quite successful with states lying on natural-parity $q\bar{q}$ Regge trajectories, such as the vector (V) mesons. On the other hand, they have always had difficulties accounting for the parameters of the pseudoscalar (P) mesons. The smallness of the pion mass, for example, is difficult to account for with a quark-gluon coupling which is also consistent with other properties of the hadron spectrum. In this paper we take the point of view that these difficulties are due to the oversimplified assumption that the long-range

part of the interaction is spin independent. We present an approach in which this assumption does not have to be made and which gives good predictions for the low-energy P - V mass differences.

In Sec. II we discuss the planar bootstrap, which is, in effect, a way of dealing with the long-range part of the interaction.² Only a subset of quark-loop diagrams are retained and a self-consistent calculation of the corresponding amplitude is made.³⁻⁵ In general this is an extremely difficult problem. In Secs. III and IV, however, we present an approach based on a simple dynamical approximation which leads to an explicit infinitely rising leading Regge trajectory α .

In Sec. V we interpret our result in terms of an effective interquark potential. If we take this potential to be energy-independent, we find that it must be of the confining type.

In Sec. VI we apply our trajectory formula to entire sets of meson + meson \rightarrow meson + meson processes in the absence of strangeness. By imposing consistency and making certain reasonable assumptions we obtain a unique solution for α_ρ and α_{K^*} corresponding to $m_\pi^2 \ll m_\rho^2$. In Sec. VII we generalize our scheme to include strangeness. We obtain a solution where we reproduce the usual additive quark-model results for the ρ , K^* , ω , ϕ , π , K , and η' , but not for the η . Finally in Sec. VIII we describe techniques for computing relative partial widths and triple-Regge couplings within our approach.

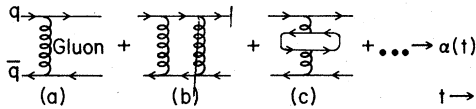


FIG. 1. The generation of the $q\bar{q}$ Regge trajectory by an infinite sum of QCD graphs.

II. BASIC DYNAMICS

One way of generating the hadron mass spectrum in a field theory such as QCD is to sum an infinite set of graphs. The usual $q\bar{q}$ mesons (M), for example, would be given by Fig. 1. This is very similar to the procedure one follows in quantum electrodynamics (QED) where, in first approximation, the positronium spectrum is given by the infinite ladder sum of Fig. 2, which is itself the Born expansion of a Bethe-Salpeter equation with a one-photon exchange potential. By solving this equation in the usual way we can then explicitly calculate the mass spectrum. The same idea underlies the quark-potential approach.

A. Quark-potential model

In a quark-potential model, Fig. 1 is rearranged as in Fig. 3, which is again the Born expansion of a Bethe-Salpeter (or Schrödinger) equation, whose solution gives the spectrum.⁶ At very short distances the potential V is dominated by the one-gluon exchange graph of Fig. 1(a) (asymptotic freedom), similar to the one-photon exchange of Fig. 2(a). At larger distances V is much more complicated but is believed to be dominated by infrared singularities which give $V \rightarrow \infty$ as $r \rightarrow \infty$. This gives quark confinement and infinitely rising Regge trajectories, a characteristic feature of the hadron mass spectrum.

In practice, the long-range part of the potential is rarely calculated *a priori*. Instead, simple spin-independent phenomenological forms are assumed, with one or more parameters which are simply adjusted to reproduce the experimental spectrum.

In the bag model,⁷ instead of using a potential V , one sets up a Lagrangian which explicitly includes the short-range $q\bar{q}$ -gluon interaction and represents the confining long-range part of the interaction by means of a phenomenological boundary condition.

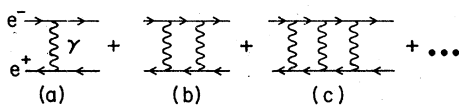


FIG. 2. The generation of the positronium spectrum by an infinite sum of photon-exchange ladder graphs.

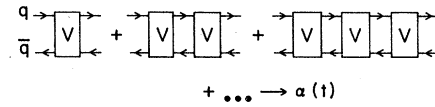


FIG. 3. Rearrangement of Fig. 1 as the Born expansion of a Bethe-Salpeter equation. The potential V is itself the sum of an infinite set of graphs.

B. Planar bootstrap

The planar bootstrap is, in effect, an explicit way of dealing with the long-range part of the interaction. Instead of using Fig. 3, one goes back to Fig. 1 and, in lowest order, retains only the "planar" graphs of Fig. 4, which have no crossed quark lines²; we have also added in the quark lines p and r at the ends of each of the graphs of Fig. 1 a procedure which does not affect the output mass spectrum. The evaluation of Fig. 4 entails a self-consistency problem (planar bootstrap), and leads to an exchange-degenerate amplitude.

By replacing quarks by antiquarks, Fig. 4 can also be used to calculate the baryon and baryonium spectrum.

It has been conjectured that Fig. 4 (with gluon lines added in) represents the $N_{\text{color}} \rightarrow \infty$, $N_{\text{flavor}} \rightarrow \infty$ limit of QCD, with $N_{\text{color}}/N_{\text{flavor}}$ finite.⁸ In a purely S -matrix theory, it represents the $N_{\text{flavor}} \rightarrow \infty$ limit of all quark-duality graphs; once we know the solution of the planar bootstrap the effect of nonplanar graphs (with crossed quark lines) can be brought in in a systematic way through a $1/N_{\text{flavor}}$ expansion.⁹

In practice, the sum of Fig. 4 can be rewritten as the infinite ladder sum of Fig. 5, which generates¹⁰ the Regge trajectory $\alpha(t)$ and in which we have the following:

(1) The requirement that there be no double counting implies that the a, b, c, \dots cluster masses are bounded. They are therefore dominated by bound states and resonances and will be approximated by single narrow peaks.

(2) The wavy lines in Figs. 5(b), 5(c), \dots are usually approximated by Regge exchanges. In principle, however, they should themselves be infinite ladder sums of the form of the entire sum of Fig. 5.

Figure 4 implies duality,¹¹ so that we must have the finite-energy sum-rule constraint of Fig. 6.

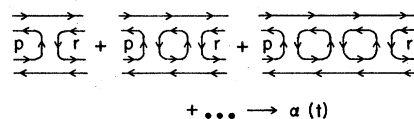


FIG. 4. The sum of planar quark-loop graphs for a meson + meson \rightarrow meson + meson process. In QCD, we must also add in gluon lines.

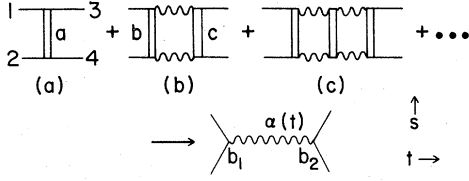


FIG. 5. The generation of the Regge trajectory α by an infinite sum of ladder graphs corresponding to the topological structure of Fig. 4. We will represent this by $12(a)34 \rightarrow \alpha$ if 1 and 2 are particles and by $\alpha_1\alpha_2(a)34 \rightarrow \alpha$ if they are Reggeons.

The external lines of Figs. 5 and 6 could themselves be Reggeons.

In what follows we will represent the process of Fig. 5 by

$$12(a)34 \rightarrow \alpha \quad (2.1)$$

if 1 and 2 are particles, and by

$$\alpha_1\alpha_2(a)34 \rightarrow \alpha \quad (2.2)$$

if they are members of the Regge families α_1 and α_2 . In the latter case their spins are given by

$$S_i = \alpha_i(m_i^2), \quad i=1,2, \quad (2.3)$$

where S_i and m_i are the spin and mass of particle i .

III. SUM OF LADDER GRAPHS

In what follows we will deal with the "ordered" planar amplitude $T(s,t)$, which only has s - t crossing.² The full planar amplitude is then a linear combination of $T(s,t)$, $T(s,u)$, and $T(t,u)$, where s, t, u are the usual Mandelstam variables. We shall define our amplitudes so that they have a Regge behavior $s^{\alpha(t)}$. In the case of lower-helicity amplitudes this may mean that we have to multiply them by appropriate polynomials in s (for an explicit example see Appendix C).

A. A representation for the projected absorptive part

We can achieve a partial diagonalization of the t -channel planar unitarity satisfied by the sum of Fig. 5 by using the usual Froissart-Gribov partial-wave projection¹⁰

$$T_j(t) = (2\pi q_i q_f)^{-1} \int_0^\infty ds A Q_j(\cos\theta_t),$$

$$\int \left(\begin{array}{c} 1 \text{---} 3 \\ | \quad | \\ a \\ | \quad | \\ 2 \text{---} 4 \end{array} \right) = \int \left(\begin{array}{c} \alpha(t) \\ / \quad \backslash \\ b_1 \quad b_2 \end{array} \right)$$

FIG. 6. Average duality relation between cluster a and Reggeon $\alpha(t)$.

where A is the s -channel absorptive part, normalized so $A = \text{Im} T$ for $t < 0$, while q_i and q_f are the initial and final three-momenta and θ_t is the scattering angle in the t -channel c.m. system. In general T_j has kinematic threshold singularities, which can be removed by using $\tilde{T}_j = (q_i q_f)^{-j} T_j$ instead of T_j itself. Now

$$\cos\theta_t = \frac{1}{2q_i q_f} \left[\nu + \frac{(m_1^2 - m_2^2)(m_3^2 - m_4^2)}{2t} \right],$$

where $\nu = \frac{1}{2}(s - u)$, which can also be written as

$$\nu = s + \frac{1}{2} \left(t - \sum_{i=1}^4 m_i^2 \right). \quad (3.1)$$

If we therefore make the usual expansion of $z^{j+1} Q_j(z)$ in powers of z^{-2} and expand in powers of $1/t$, we obtain

$$\tilde{T}_j(t) = \sum_{k=0}^{\infty} \sum_{h=0}^{\infty} c_{kh}(j) \left[\frac{(m_1^2 - m_2^2)(m_3^2 - m_4^2)}{2t} \right]^k \times (q_i q_f)^{2h} A_{j+h+2h}(t), \quad (3.2)$$

where

$$A_j(t) = \int_0^\infty ds A(\nu, t) \nu^{-j-1}. \quad (3.3)$$

This $Q_j(\cos\theta_t)$ expansion is known to converge quite rapidly for $|\cos\theta_t| > 1$. Of course, Equation (3.3) becomes meaningless if t is such that we can have $\nu = 0$ within its integral.

In most cases, especially when we are only calculating leading trajectories, we can approximate \tilde{T}_j by the first term in the double sum (3.2). When $m_1 \neq m_2$ or $m_3 \neq m_4$, however, $q_i q_f$ is infinite and the higher terms in Eq. (3.2) have infinite coefficients at $t = 0$. This difficulty is related to the need for $j = \alpha - 1, \alpha - 2, \dots$ daughter poles at $t = 0$ for such processes.¹⁰ One way of dealing with it is to use $A_j(t)$ instead of $\tilde{T}_j(t)$ in our calculations. However, $A_j(t)$ does not have the desirable partial diagonalization of planar unitarity property that $T_j(t)$ or $\tilde{T}_j(t)$ have.

Because of the above complication we shall restrict ourselves to equal-mass channels with $m_1 = m_2, m_3 = m_4$. In this case only the $k = 0$ terms of Eq. (3.2) contribute and the remaining $A_j, A_{j+2}, A_{j+4}, \dots$ terms have finite coefficients. We can therefore safely make the approximation

$$\tilde{T}_j(t) \approx c_{00}(j) A_j(t),$$

which permits us to use the Mellin transform (3.3) as our basic projection from now on.

If we associate a coupling-strength parameter φ with each of the clusters a, b, c, \dots , the sum of Fig. 5 now has the form

$$A_j(t) = \varphi a_j^{(1)}(t) + \varphi^2 a_j^{(2)}(t) + \varphi^3 a_j^{(3)}(t) + \dots \quad (3.4)$$

If we assume that the cluster a can be approximated by a single narrow peak of mass $\sqrt{s_a}$, Fig. 5(a) gives a contribution to $A(\nu, t)$ of

$$\varphi a^{(1)}(\nu, t) = \Gamma(t)\delta(s - s_a). \quad (3.5)$$

Taking the Mellin transform (3.3) we then obtain

$$\varphi a_j^{(1)}(t) = \Gamma(t)\nu_a^{-j-1}, \quad (3.6)$$

where

$$\nu_h = s_h + \frac{1}{2} \left(t - \sum_{i=1}^4 m_i^2 \right) \quad (3.7)$$

with $h = a$. The remaining terms in Fig. 5 involve difficult loop integrals. An approximate way of dealing with them will be presented in Sec. IV.

We can rewrite Eq. (3.4) in the form

$$A_j = \frac{\varphi a_j^{(1)}}{1 - K(j)}, \quad (3.8)$$

where

$$K(j) = \varphi \frac{a_j^{(2)}}{a_j^{(1)}} + \varphi^2 \left[\frac{a_j^{(3)}}{a_j^{(1)}} - \left(\frac{a_j^{(2)}}{a_j^{(1)}} \right)^2 \right] + \dots \quad (3.9)$$

This φ expansion generally converges much more rapidly than the original series (3.4). (See, for example, the factorizable model below.) If we use Eq. (3.3) we find, order by order, that Eq. (3.9) has the structure

$$K(j) = \int_{\nu_0/\nu_a}^{\infty} dy y^{j-1} G(y), \quad (3.10)$$

where ν_0 is related to the threshold $s = s_0$ of Fig. 5(b) through Eq. (3.7) with $s_h = s_0$.

From Eq. (3.8), $A_j(t)$ has a j pole at $j = \alpha$ if

$$K(\alpha) = 1. \quad (3.11)$$

The corresponding residue (see Fig. 5) is

$$b_1 b_2 = -\varphi a_\alpha^{(1)} / K'(\alpha). \quad (3.12)$$

B. A factorizable-model example

In the case of a factorizable model we have

$$\begin{aligned} \varphi a_j^{(1)} &= u_j v_j, \\ \varphi^2 a_j^{(2)} &= u_j k_j v_j, \\ \varphi^3 a_j^{(3)} &= u_j k_j k_j v_j, \text{ etc.}, \end{aligned} \quad (3.13)$$

and Eq. (3.9) reduces to

$$K(j) = k_j = \varphi a_j^{(2)} / a_j^{(1)}. \quad (3.14)$$

Thus the series (3.9) not only converges rapidly, but actually truncates after the first term. From Eqs. (3.3), (3.6), and (3.14) we see directly that $K(j)$ has the structure (3.10) with

$$G(\nu/\nu_a) = \varphi^2 \nu_a a^{(2)}(\nu, t) / \Gamma(t). \quad (3.15)$$

Finally, we have t -channel unitarity as long as

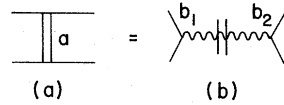


FIG. 7. Duality replacement of cluster exchange (a) by Regge behavior with an upper cutoff in s or with a modified propagator.

$$A_j \approx c_{00}^{-1} \bar{T}_j.$$

Factorizable models of the type given by Eq. (3.13) arise quite naturally if we have average duality (Fig. 6). Crudely speaking, this permits us to replace cluster exchange by Regge behavior with an upper cutoff in s (Ref. 11) (Fig. 7). A more refined version¹² is to use what amounts to a modified Regge propagator in Fig. 7(b). In either case, Fig. 7(b) then has a factorized form which permits us to replace Fig. 5 by Fig. 8 which, in turn, gives us Eq. (3.13), if we make the usual kinematic approximations.

Another way in which we can obtain Eqs. (3.8) and (3.14), even when we do not have a factorizable model, is to write down the $[1, 1]$ Padé approximant of the series (3.4).^{5,12} Such a diagonal approximant will have t -channel unitarity as long as $A_j \approx c_{00}^{-1} \bar{T}_j$.

IV. DUALITY AND AN EXPLICIT REGGE TRAJECTORY

We will now combine the expressions of Sec. III with the finite-energy sum rule of Fig. 6. This sort of duality constraint on sums of ladder graphs was first used a number of years ago in a pion exchange model¹³ and has more recently been used extensively in dual-unitarization calculations.¹¹ If we then make a certain simple dynamical approximation and impose uniqueness, we obtain an explicit algebraic expression¹⁴ for the Regge trajectory $\alpha(t)$.

A. Finite-energy sum rules

With the normalization of Eq. (3.12), $A(\nu, t)$ has the Regge behavior $b_1 b_2 \nu^\alpha$ for large s , and Fig. 6 corresponds to the finite-energy sum rule¹⁵

$$\int_0^{\bar{s}} ds [\varphi a^{(1)}(\nu, t) - b_1 b_2 \nu^{\alpha(t)}] \nu^{-s} \Gamma^{-s_2} = 0 \quad (4.1)$$

for the highest-helicity amplitude. Our labeling

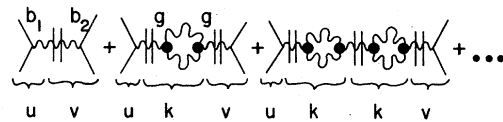


FIG. 8. Reduction of Fig. 5 to a factorizable form, using Fig. 7.

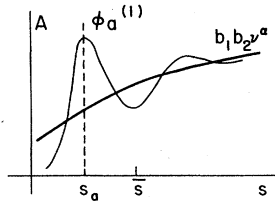


FIG. 9. Regge-resonance duality for the absorptive part A.

in Fig. 6 is such that the spin sum

$$S_1 + S_2 \geq S_3 + S_4. \quad (4.2)$$

(See Appendix C for a more detailed treatment in the simple case of $N\bar{N} \rightarrow \pi\pi$.) Similar rules apply for lower-helicity amplitudes, where we have to make the replacement

$$S_1 + S_2 \rightarrow S_1 + S_2 - n, \quad n = \text{integer} > 0. \quad (4.3)$$

We shall not consider these in the present paper.

In most applications \bar{s} is taken approximately midway between s_a and the next peak above it (See Fig. 9). Equations (4.1) and (3.5) would then give

$$\Gamma(t) = \frac{b_1 b_2 \nu_a^{\alpha+1}}{\alpha + 1 - S_1 - S_2} \left(\frac{\bar{\nu}}{\nu_a} \right)^{\alpha+1-S_1-S_2}, \quad (4.4)$$

where $\bar{\nu} = \bar{s} + \frac{1}{2}(t - \sum m_i^2)$. If, on the other hand, we assume an even more local version of duality and take $\bar{\nu} = \nu_a$ (or $\bar{s} = s_a$), we must only include a fraction $f^{-1} \approx \frac{1}{2}$ of the $\phi_a^{(1)}$ peak of Fig. 9 when we evaluate the integral of Eq. (4.1). Using the approximation (3.5) we then have

$$\int_0^{s_a} ds \phi_a^{(1)} \nu^{-S_1-S_2} = f^{-1} \Gamma \nu_a^{-S_1-S_2},$$

and so Eq. (4.1) gives

$$\Gamma(t) = \frac{b_1(t) b_2(t) \nu_a^{\alpha+1}}{\alpha(t) + 1 - S_1 - S_2} f. \quad (4.5)$$

If we combine this with Eqs. (3.6), (3.10), (3.11), and (3.12), we obtain

$$\alpha(t) = S_1 + S_2 - 1 + f \frac{\int_{\nu_0/\nu_a}^{\infty} dy y^{-\alpha-1} G(y)}{\int_{\nu_0/\nu_a}^{\infty} dy y^{-\alpha-1} G(y) \ln y}, \quad (4.6)$$

where $y = \nu/\nu_a$.

B. Dynamical approximations

The function $y^{-\alpha-1}G(y)$ typically has the form shown in Fig. 10 for $\alpha \geq \alpha_c$, where α_c is the usual branch point in j associated with two-Reggeon exchange. For example, since Fig. 5(b) gives

$$\varphi^2 a^{(2)} \propto \nu^\alpha \epsilon^{\gamma} \quad (4.7)$$

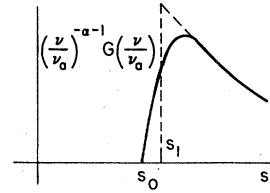


FIG. 10. Plot of $y^{-\alpha-1}G(y)$ vs s (solid curve) where $y = \nu/\nu_a$. For a factorizable model, G is given by Eq. (3.15). The dashed curve is a plot of the approximate form (4.10).

for moderately large ν , the factorizable model of Eqs. (3.13) and (3.15) gives

$$y^{-\alpha-1}G(y) \propto \nu^\alpha \epsilon^{\alpha+\gamma-1}. \quad (4.8)$$

We have neglected $\ln \nu$ factors, whose effect can be approximately absorbed into the constant γ . If we replace the wavy lines of Fig. 5(b) by infinite ladder sums, Eq. (4.7) is no longer a good description in the limit $\nu \rightarrow \infty$ because of the usual Mandelstam cut-cancellation arguments.¹⁰ However, we might still expect Eq. (4.7) to hold for moderate values of ν , which is in fact the only region which is relevant for our considerations.

Since Fig. 5(c), ... are also two-Reggeon-exchange graphs, Eq. (4.8) should continue to be valid even if we do not have a factorizable model as long as the series (3.9) converges for $j \geq \alpha_c + \gamma$.

For $\alpha \geq \alpha_c + \gamma$, Eq. (4.8) corresponds to a rapid falloff for large s and hence to a peaking of $y^{-\alpha-1}G(y)$ near its threshold (see Fig. 10). This permits us to make the rather crude approximation

$$\ln y \approx \ln(\nu_0/\nu_a) \quad (4.9)$$

within the denominator integral of Eq. (4.6). We then obtain an explicit algebraic expression for $\alpha(t)$ independent of the specific form of $G(y)$. This was the expression used in Refs. 14-16. Its main defect is that it ignores the large- ν tail in Fig. 10. It is also incapable of accounting for the ρ - π mass difference, as we shall see.

An improved approximation, which we shall use from now on and which does include the effect of a large- ν tail in Fig. 10, is to take

$$G(y) \propto y^\lambda \theta\left(y - \frac{\nu_1}{\nu_a}\right), \quad (4.10)$$

where θ is the usual step function, ν_1 is given by Eq. (3.7) with $k=1$, and s_1 is a point slightly above the threshold s_0 (see Fig. 10). Equation (4.6) then gives

$$[\alpha(t) + 1 - S_1 - S_2] \left[\ln\left(\frac{\nu_1}{\nu_a}\right) - \frac{1}{\lambda - \alpha(t)} \right] = f. \quad (4.11)$$

Equation (4.10), of course, amounts to using the asymptotic two-Reggeon-exchange form (4.8) down to an effective threshold at $s = s_1$, so that

$$\lambda = \alpha_c + \gamma. \quad (4.12)$$

Equations (4.4), (4.5), (4.11), and (4.12) give

$$\alpha(t) - \alpha_c(t) - \gamma = \left[\frac{f}{\tilde{f}} \ln\left(\frac{\nu}{\nu_a}\right) - \ln\left(\frac{\nu_0}{\nu_a}\right) \right]^{-1} \quad (4.13)$$

and

$$\alpha(t) = S_1 + S_2 + L\left(\frac{\nu_a}{s_1 - s_a}\right), \quad (4.14)$$

where

$$L(x) = \frac{\tilde{f}}{\ln(1+x^{-1})} - 1 \quad (4.15)$$

and $\tilde{f} = \ln f$. Note that Eqs. (4.14) and (4.15) give exactly the same functional form for $\alpha(t)$ as the threshold-peak approximation of Eqs. (4.9) and (4.6) but with f replaced by \tilde{f} .

Equations (4.14) and (4.15) give an $\alpha(t)$ which is approximately linear in t (see below). This, in turn, implies an approximately linear $\alpha_c(t)$, and so

$$\alpha'_c(t)/\alpha'(t) \approx \xi = \text{constant}. \quad (4.16)$$

If the Regge trajectories exchanged in Figs. 5(b), 5(c), ... have the same slope as the output $\alpha(t)$, as will be true in all the cases considered below, then $\xi = \frac{1}{2}$.

Equations (4.13) and (4.16) are consistent with Eqs. (4.14) and (4.15) only if

$$\bar{s} = s_1, \quad \ln f = \tilde{f} = f - (1 - \xi)^{-1}. \quad (4.17)$$

The first result is physically reasonable if we attribute the generation of the Regge behavior in Eq. (4.1) to Figs. 5(b), 5(c), If $\xi = \frac{1}{2}$, the second result gives

$$f = 3.147, \quad \tilde{f} = 1.147. \quad (4.18)$$

C. Trajectory properties

From Eqs. (4.14) and (4.15) we see that $\alpha(t)$ has singularities at $\nu_a = 0$ and $\nu_1 = 0$, which can be joined by a cut. Our use of the Mellin transform is invalid for $\nu = \nu_a \leq 0$, however, as we saw in Sec. III. The $\alpha(t)$ singularities thus occur in a region where our model is expected to fail anyway.

Equations (4.14) and (4.15) give an approximately linear $\alpha(t)$ in the entire range $\nu_a \gtrsim 0$. We shall therefore make the linear approximation

$$L(x) \approx c + \gamma x, \quad (4.19)$$

where c and γ are pure numbers adjusted so that

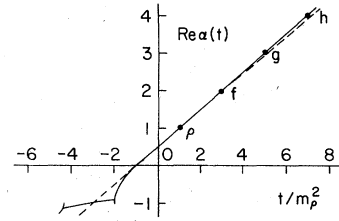


FIG. 11. Plot of $\text{Re}\alpha(t)$ as given by Eqs. (4.14) and (4.15) (solid line) and (4.14), (4.19), and (4.20) (dashed line) for $\pi\pi$ scattering with $m_\pi^2 = 0$, $\tilde{f} = 1.147$, $s_a = m_\rho^2$ and s_1 adjusted so $\alpha(s_a) = 1$.

$L(1)$ and $L'(\infty)$ are exactly reproduced. This gives

$$c = \left(\frac{1}{\ln 2} - 1\right) \tilde{f} - 1, \quad \gamma = \tilde{f}. \quad (4.20)$$

Figure 11 gives a plot (solid line) of the trajectory given by Eqs. (4.14) and (4.15) for $\pi\pi$ scattering with $m_\pi^2 \approx 0$, $\tilde{f} = 1.147$, $s_a = m_\rho^2$ and s_1 adjusted so $\alpha(s_a) = 1$. This is compared with the linear approximation (dashed line) given by Eqs. (4.14), (4.19), and (4.20). We find that the resonance masses are the same to within 1% of their values.

We shall see below that consistency between different processes is best achieved by using the linear form (4.19), rather than the nonlinear form given by Eq. (4.15). (Actually the latter can also be made exactly linear by giving s_1 a very slight x dependence.) We shall therefore use the linear form (4.19) from now on, and assume that it can be extrapolated to the region $\nu_a \leq 0$.

V. SIMPLE EQUIVALENT-POTENTIAL PICTURE AND "EFFECTIVE CONFINEMENT"

For simplicity let us consider a process where all of the external masses m_i in Fig. 5 are equal. Equation (3.7) then gives $\nu_a = s_a + 2q_t^2$ and so, from Eq. (4.19),

$$L\left(\frac{\nu_a}{s_1 - s_a}\right) \approx c + 2\alpha' s_a + 4\alpha' q_t^2, \quad (5.1)$$

where q_t is the relativistic c.m. three-momentum in the t channel. Since $\alpha = J$ in Eq. (4.14) we now see *a posteriori* that L plays the role of an orbital angular momentum which can be reproduced by an effective Schrödinger equation

$$-\nabla^2 \psi + 2mV\psi = q_t^2 \psi, \quad (5.2)$$

with an equivalent energy-dependent potential $V = V(r, q_t^2)$.

Instead of considering hadron-hadron scattering, suppose we next consider effective $q\bar{q}$ "scattering," as in Figs. 1 and 3. At the planar level this would be given by Fig. 4 with the quark lines p and r re-

moved. This does not, of course, change $\alpha(t)$, which can therefore again be reproduced by the effective Schrödinger equation (5.2). In this case, however, we shall follow the usual practice of taking the (interquark) potential V to be energy independent (static), so $V = V(r)$. If we assume that this is in fact the case, the linear form (5.1) is then reproduced by the effective harmonic-oscillator potential

$$V(r) = \frac{1}{8m\alpha'} \left[\left(\frac{3}{2} + c + 2\alpha' s_a \right) + \frac{r^2}{16\alpha'^2} \right], \quad (5.3)$$

which is a confining potential. This result depends critically on our using a static potential, an assumption which we have not really justified.

It is straightforward to generalize the above results to the case where the external masses m_i are not all equal, although the resulting effective potentials may be more complicated in this case. Instead of Eq. (5.2) we could also use an effective Bethe-Salpeter equation, or a Lagrangian with a relativistic boundary condition⁷ (bag model). The qualitative conclusions are the same.

VI. MESON MASS SPECTRUM IN THE ABSENCE OF STRANGENESS

If we combine Eqs. (3.7), (4.14), (4.19), and (4.20) we obtain

$$\alpha(t) = S_1 + S_2 + c + \alpha' \left(2s_a + t - \sum_{i=1}^4 m_i^2 \right), \quad (6.1)$$

with

$$\alpha' = \frac{1}{2} \tilde{f} (s_1 - s_a)^{-1}. \quad (6.2)$$

Now $\alpha(t)$ must be independent of the particular process we consider. This is not automatically true of Eq. (6.1). If, however, we impose this requirement, we obtain powerful self-consistency conditions on the parameters of the model.¹⁶ Suppose, for example, we take $a = \rho$ in Fig. 5 for both $\pi\pi \rightarrow \pi\pi$ and $\rho\rho \rightarrow \rho\rho$, an assumption which we shall justify below. Now $S_\pi = 0$ and $S_\rho = 1$ and so we must have $m_\rho^2 - m_\pi^2 = (2\alpha')^{-1}$ if Eq. (6.1) is to generate the same $\alpha = \alpha_\rho$ for both processes.

We can obtain simultaneous consistency for entire sets of meson + meson \rightarrow meson + meson processes if we make the following reasonable assumptions:

(a) The lowest members of leading Regge families are the same as in conventional quark models. This is not really an additional assumption if we think of our model as being itself a type of quark model, in the sense discussed in Secs. II and V.

(b) The mass $\sqrt{s_a}$ of the cluster a in Fig. 5 should be as low as possible consistent with other channels. The suppression of higher masses is a

property of more specific models of this type and is consistent with property (1) of Sec. IIB. We also find (*a posteriori*) that it is needed to guarantee that \bar{s} be approximately halfway between two actual resonances, as required by semilocal duality.

(c) As many channels should couple to a given trajectory as possible; in other words, we will not take allowed couplings = 0 unless we are forced to do so by consistency. As discussed in Sec. III, however, we will restrict ourselves to equal-mass channels with $m_1 = m_2$, $m_3 = m_4$, since we were unable to find a reliable expression for $\alpha(t)$ in the case where $m_1 \neq m_2$ or $m_3 \neq m_4$. [A somewhat different set of assumptions was used in Ref. 16 in the case of exact SU(3) symmetry.]

A. V trajectory

In the absence of strangeness the lowest $q\bar{q}$ states are $V = (\rho, \omega)$ and $P = (\pi, \eta_u)$, where $\eta_u = (i\bar{u}\bar{u} + d\bar{d})/\sqrt{2}$. These lie on the trajectories α_V and α_P . For the time being we will assume the usual quark-model result that $m_V = m_\rho = m_\omega$ and $m_P = m_\pi = m_\eta$.

Using the notation of Eq. (2.1) the only equal-mass-channel processes involving P and V and generating α_V are

$$P P(a_1) P P \rightarrow \alpha_V, \quad (6.3)$$

$$V V(a_2) P P \rightarrow \alpha_V, \quad (6.4)$$

$$V V(a_3) V V \rightarrow \alpha_V. \quad (6.5)$$

Now G parity excludes any P contribution to the a_1 cluster. If we impose the requirement (b) that the masses of a_1 , a_2 , and a_3 be as low as possible, Eq. (6.1) and consistency requires us to take

$$s_{a_1} = m_V^2, \quad s_{a_2} = m_P^2, \quad s_{a_3} = m_V^2. \quad (6.6)$$

Note that it is consistent to exclude contributions to the clusters from higher states such as V^* , the $j=2$ Regge recurrence of V . If we did include them, we would be double-counting when we add Figs. 5(a) and 5(b), since Eq. (6.2) gives $s_1 - s_a = \frac{1}{2} \tilde{f} \alpha_V'^{-1}$ which is smaller than the trajectory spacing α'^{-1} if \tilde{f} is given by Eq. (4.18) (see Fig. 10).

Using Eqs. (6.1) and (6.6), consistency between Eqs. (6.3) and (6.4) gives an $\alpha_V = \alpha_P = \alpha_\omega$ with

$$\alpha'_\rho = (1+c)m_\rho^{-2}, \quad (6.7)$$

$$\alpha_\rho(0) = -c, \quad (6.8)$$

$$m_\pi^2 = m_\rho^2 - (2\alpha'_\rho)^{-1}. \quad (6.9)$$

Equations (4.18) and (4.20) give $c \approx -0.5$ and so Eqs. (6.7)–(6.9) give

$$\alpha'_\rho \approx \frac{1}{2} m_\rho^{-2} = 0.83 \text{ GeV}^{-2}, \quad \alpha_\rho(0) \approx 0.5, \quad m_\pi^2 \approx 0, \quad (6.10)$$

in good agreement with experiment. The smallness of m_r^2 depends critically on our value of c , which could not have been obtained if we had used the approximation (4.9), as in Refs. 14-16.

Equations (4.20), (6.7), and (6.2) give

$$s_1 = s_a + \frac{1}{2} m_\rho^2 \left(\frac{1}{\ln 2} - 1 \right)^{-1} \approx 2.13 m_\rho^2.$$

This means that the clusters b and c in Fig. 5 must include a substantial P contribution, since we would otherwise have $s_1 > s_0 = 4m_\rho^2$, which would then be the threshold of Fig. 5(b) (see Fig. 10).

B. P trajectory

If we use Eq. (6.1) and the results (6.6)-(6.9) we find that

$$\alpha_V \alpha_V (a_2) PP \rightarrow \alpha_V, \quad (6.11)$$

$$\alpha_V \alpha_V (a_3) VV \rightarrow \alpha_V \quad (6.12)$$

are automatically satisfied. On the other hand, if we apply Eq. (6.1) to

$$\alpha_P \alpha_P (a_1) PP \rightarrow \alpha_V, \quad (6.13)$$

we find that we must have an $\alpha_P = \alpha_r = \alpha_{\eta_u}$ with

$$\alpha_r' = \alpha_p', \quad (6.14)$$

which, when combined with Eq. (6.9), gives

$$\alpha_r(t) = \alpha_p(t) - \frac{1}{2}, \quad (6.15)$$

in good agreement with experiment. At $t \approx 0$ it also agrees with the result obtained by imposing the Adler-zero condition on either the Lovelace-Veneziano model¹⁷ or a class of multiperipheral models.¹⁸

The only equal-mass-channel process generating α_P which is consistent with the quantum numbers involved is now

$$\alpha_V \alpha_V (a_4) VV \rightarrow \alpha_P. \quad (6.16)$$

Using Eq. (6.1) consistency with Eq. (6.15) gives

$$s_{a_4} = m_r^2 + \frac{1}{2}(m_\rho^2 - m_r^2). \quad (6.17)$$

This does not correspond to any single state but is rather on average of the P and V , both of which can contribute to a_4 .

C. Additional processes and trajectories

In addition to the processes corresponding to Eq. (6.12) we can also have, subject to the constraint (4.2),

$$\alpha_V \alpha_V (a_3^r) V^r V^r \rightarrow \alpha_V, \quad (6.18)$$

$$\alpha_V \alpha_V (a_3^{rr}) V^{rr} V^{rr} \rightarrow \alpha_V, \text{ etc.}, \quad (6.19)$$

where a_3^r, a_3^{rr}, \dots have the same masses as V^r ,

V^{rr}, \dots , the $j=2, 3, \dots$ Regge recurrences of V . On the other hand, if we do insist on $s_a = m_V^2$ in Eq. (6.18), the leading output trajectory will be $\alpha = \alpha_V - 2$. This means that the coupling $V^r V^r \alpha_V = 0$, which, in turn implies that $V^r V^r V = 0$, a result which is not consistent with taking $s_a = m_V^2$ in the first place. Similar considerations apply to Eq. (6.19) and to processes in which we replace PP by $P^r P^r, P^{rr} P^{rr}$, etc., in Eqs. (6.11) and (6.13).

Our model was based on the assumption that $A = b_1 b_2 \nu^\alpha$ on the average. Since $\nu \propto \cos \theta_t$ when $m_1 = m_2$ or $m_3 = m_4$, this means that, when $\alpha = \text{integer}$, we not only have a leading-trajectory state with angular momentum $J = \alpha$, but also daughters with $J = \alpha - 2, \alpha - 4, \dots$. Of course, to actually verify the $A = b_1 b_2 \nu^\alpha$ assumption *a priori*, we have to go to a much more detailed model than the one considered here.

VII. MESON MASS SPECTRUM IN THE PRESENCE OF STRANGENESS

In the limit of exact SU(3) with degenerate $V = (\rho, K^*, \omega, \phi)$ and $P = (\pi, K, \eta_u, \eta_s = s\bar{s})$, all of the results of the preceding section continue to apply; here K stands for (K, \bar{K}) and K^* for (K^*, \bar{K}^*) . In this section we shall see that a solution satisfying the assumptions (a)-(c) of Sec. VI can also be found when the symmetry is broken and m_ρ and m_{K^*} are *required* to have different masses.

A. Processes with α_V outputs

The equal-mass-channel processes corresponding to Eq. (6.13) are now

$$\alpha_r \alpha_r (a_{11}) \pi\pi \rightarrow \alpha_\rho, \quad (7.1a)$$

$$\alpha_K \alpha_K (a_{12}) KK \rightarrow \alpha_\rho, \quad (7.1b)$$

$$\alpha_K \alpha_K (a_{13}) KK \rightarrow \alpha_\omega, \quad (7.1c)$$

$$\alpha_K \alpha_K (a_{14}) \pi\pi \rightarrow \alpha_\rho, \quad (7.1d)$$

$$\alpha_K \alpha_K (a_{15}) KK \rightarrow \alpha_\phi, \quad (7.1e)$$

and those corresponding to Eq. (6.11) are

$$\alpha_\rho \alpha_\rho (a_{21}) \pi\pi \rightarrow \alpha_\rho, \quad (7.2a)$$

$$\alpha_{K^*} \alpha_{K^*} (a_{22}) KK \rightarrow \alpha_\rho, \quad (7.2b)$$

$$\alpha_{K^*} \alpha_{K^*} (a_{23}) KK \rightarrow \alpha_\omega, \quad (7.2c)$$

$$\alpha_{K^*} \alpha_{K^*} (a_{24}) \pi\pi \rightarrow \alpha_\rho, \quad (7.2d)$$

$$\alpha_{K^*} \alpha_{K^*} (a_{25}) KK \rightarrow \alpha_\phi. \quad (7.2e)$$

If we require these processes to simultaneously satisfy Eq. (6.1) and the requirement (b) of Sec. VI that the cluster masses be as low as possible, we find that, with $m_{K^*} > m_\rho$, we have

$$s_{a_{11}} = m_\rho^2, \quad s_{a_{12}} = s_{a_{13}} = m_\phi^2, \quad s_{a_{14}} = m_{K^*}^2, \quad (7.3)$$

$$s_{a_{15}} = m_\rho^2 + \epsilon, \quad \epsilon \geq 0 \quad (7.4)$$

$$s_{a_{21}} = m_\tau^2, \quad s_{a_{22}} = s_{a_{23}} = m_{\eta_s}^2, \quad s_{a_{24}} = m_K^2 \quad (7.5)$$

$$s_{a_{25}} = m_\tau^2 + \epsilon, \quad \epsilon \geq 0. \quad (7.6)$$

We then have

$$\alpha'_\rho = \alpha'_\omega = \alpha'_{K^*} = \alpha'_\tau = \alpha'_K \quad (7.7)$$

and the familiar mass formulas

$$m_\phi^2 - m_{K^*}^2 = m_{K^*}^2 - m_\rho^2 = m_K^2 - m_\tau^2 = m_{\eta_s}^2 - m_K^2, \quad (7.8)$$

$$m_\omega = m_\rho. \quad (7.9)$$

Equations (6.7)–(6.10) are also reproduced.

The quantum-number requirement that $\epsilon \geq 0$ for all of the processes represented by Eqs. (7.1e) and (7.2e) forces us to take $\alpha'_\phi \geq \alpha'_K$. If, in addition, we require that the mass of a_{15} stays bounded for all of these processes we must have

$$\epsilon = m_{K^*}^2 - m_\rho^2, \quad \alpha'_\phi = \alpha'_K. \quad (7.10)$$

In other words, in order to have symmetry breaking with $m_{K^*} > m_\rho$, a_{15} and a_{25} must have slight admixtures of higher states in addition to the ρ and π , respectively. Presumably such admixtures could even come from nonplanar effects, which would then be the mechanism for inducing our symmetry breaking.

Finally the equal-mass-channel processes corresponding to Eq. (6.12) are now

$$\alpha_\rho \alpha_\rho (a_{31}) \rho \rho \rightarrow \alpha_\rho, \quad (7.11a)$$

$$\alpha_{K^*} \alpha_{K^*} (a_{32}) K^* K^* \rightarrow \alpha_\rho, \quad (7.11b)$$

$$\alpha_{K^*} \alpha_{K^*} (a_{33}) K^* K^* \rightarrow \alpha_\omega, \quad (7.11c)$$

$$\alpha_{K^*} \alpha_{K^*} (a_{34}) \rho \rho \rightarrow \alpha_\rho, \quad (7.11d)$$

$$\alpha_{K^*} \alpha_{K^*} (a_{35}) K^* K^* \rightarrow \alpha_\phi. \quad (7.11e)$$

Using Eq. (6.1), consistency with the processes (7.1) and (7.2) now gives

$$s_{a_{3i}} = s_{a_{1i}}, \quad i = 1, 2, \dots, 5. \quad (7.12)$$

Processes of the type discussed in Sec. VIC also continue to be valid in this case.

B. Processes with α_ρ outputs

The equal-mass-channel processes corresponding to Eq. (6.16) are now

$$\alpha_\rho \alpha_\omega (a_{41}) \omega \rho \rightarrow \alpha_\tau, \quad (7.13a)$$

$$\alpha_\rho \alpha_\rho (a_{42}) \rho \rho \rightarrow \alpha_{\eta_u}, \quad (7.13b)$$

$$\alpha_\omega \alpha_\omega (a_{43}) \omega \omega \rightarrow \alpha_{\eta_u}, \quad (7.13c)$$

$$\alpha_{K^*} \alpha_{K^*} (a_{44}) K^* K^* \rightarrow \alpha_\tau, \quad (7.13d)$$

$$\alpha_{K^*} \alpha_{K^*} (a_{45}) K^* K^* \rightarrow \alpha_{\eta_u}, \quad (7.13e)$$

$$\alpha_{K^*} \alpha_{K^*} (a_{46}) K^* K^* \rightarrow \alpha_{\eta_s}, \quad (7.13f)$$

If we require these processes to simultaneously satisfy Eq. (6.1) and the requirement (b) of Sec. VI that the cluster masses be as low as possible, we find that, with the parameters obtained in the previous subsection, we must have

$$s_{a_{41}} = m_\tau^2 + \frac{1}{2}(m_\rho^2 - m_\tau^2), \quad (7.14a)$$

$$s_{a_{42}} = s_{a_{43}} = m_{\eta_u}^2, \quad (7.14b)$$

$$s_{a_{44}} = m_{\eta_s}^2 + \frac{1}{2}(m_\rho^2 - m_\tau^2), \quad (7.14c)$$

$$s_{a_{45}} = m_{\eta_s}^2 + \frac{1}{3}(m_\rho^2 - m_\tau^2), \quad (7.14d)$$

$$s_{a_{46}} = m_\tau^2 + \epsilon', \quad \epsilon' \geq 0. \quad (7.14e)$$

We then have

$$\alpha'_{\eta_u} = \alpha'_\rho, \quad m_{\eta_u}^2 = \frac{1}{3}(m_\rho^2 + 2m_\tau^2), \quad (7.15)$$

which gives $m_{\eta_u} = 0.462$ GeV.

The quantum-number requirement that $\epsilon' \geq 0$ for all of the processes represented by Eq. (7.13f) forces us to take $\alpha'_{\eta_s} \geq \alpha'_{K^*}$. If, in addition, we require that the mass of a_{46} stays bounded for all of these processes we must have

$$\epsilon' = (m_{K^*}^2 - m_\tau^2) + \frac{1}{2}(m_\rho^2 - m_\tau^2), \quad \alpha'_{\eta_s} = \alpha'_{K^*}. \quad (7.16)$$

We conclude that, except for Eqs. (7.13b) and (7.13c), every one of the processes with α_ρ as output must have an admixture of higher states in addition to the lowest one in its cluster a_{4i} .

VIII. COUPLINGS

There are two kinds of couplings which can be calculated within our approach—relative partial widths and triple-Regge couplings. For simplicity we shall only consider $\pi\pi$ scattering here, but it is straightforward to generalize our approach to other processes.

A. Partial widths

Once we know $\alpha(t)$ from Eq. (6.1) we can use Eq. (4.5) to calculate the ratio $b_1 b_2 / \Gamma$. In particular if we have a model for the t dependence of $\Gamma(t)$, this gives us the t dependence of $b_1 b_2$ (see Fig. 6). If we now make a t -channel partial-wave projection of $b_1 b_2 \nu^\alpha$, we find in the usual way that we obtain a resonance of spin j at $t = t_j$ if

$$\alpha(t_j) = j. \quad (8.1)$$

With $m_\tau^2 \approx 0$, the corresponding partial width in the energy (\sqrt{t}) variable is then given by

$$\gamma_j = \frac{2^j (j+1)(j!)^2}{(2j+1)(2j)!} \left(\frac{t_j}{2s_a + t_j} \right)^{j+1} \frac{2f}{c\pi\alpha'} \frac{\Gamma(t_j)}{t_j^{3/2}}. \quad (8.2)$$

Equation (8.2) applies to the "ordered" planar amplitude $T(s, t)$ which only has s - t crossing.

For $\pi\pi$ scattering, the full planar amplitude for the t -channel isospin $I_t = 0, 1$ states is¹⁷

$$T^0 = \frac{3}{2} [T(t, s) + T(t, u)] - \frac{1}{2} T(s, u), \quad (8.3a)$$

$$T^1 = T(t, s) - T(t, u). \quad (8.3b)$$

Thus

$$\text{full partial width} = 3\gamma_j, \quad I_t = 0, \quad (8.4a)$$

$$= 2\gamma_j, \quad I_t = 1. \quad (8.4b)$$

We will assume that the cluster a in Fig. 6(a) is dominated by a $j = 1$ (ρ) resonance together with a small spinless contribution (E). With $m_\tau^2 \approx 0$, we then have

$$\Gamma(t) \approx \Gamma_1 \left[P_1 \left(1 + \frac{2t}{s_\rho} \right) + E \right]. \quad (8.5)$$

If we adjust Γ_1 so as to reproduce the experimental ρ partial width ($2\gamma_1$) of 0.155 GeV, Eq. (8.2) gives

$$3\gamma_2 = 0.122, \quad 2\gamma_3 = 0.041 \text{ GeV}, \quad \text{if } E = 0 \quad (8.6a)$$

$$3\gamma_2 = 0.111, \quad 2\gamma_3 = 0.036 \text{ GeV}, \quad \text{if } E = 0.54. \quad (8.6b)$$

The latter value of E is the one required if our model is to be crossing-symmetric at the ρ mass (see Appendix B). Equation (8.6) should be compared with the experimental f and g partial widths

$$3\gamma_2 = 0.144 \pm 0.016, \quad 2\gamma_3 = 0.043 \pm 0.007 \text{ GeV}.$$

We should keep in mind, however, that the f may be strongly modified by nonplanar cylinder corrections.

B. Triple-Regge coupling

The above procedure only gives coupling ratios. The condition (3.11), on the other hand, gives us information on the overall magnitudes of couplings. In general, extracting this information can be quite difficult.^{4,5} Things simplify considerably if $K(j)$ is given by Eq. (3.14). If $a_j^{(2)}$ is given by Fig. 8(b), for instance, and $a_j^{(1)}$ by Fig. 8(a), we see that $b_1 b_2$ cancels out in the ratio (3.14). Equation (3.11) then gives a condition on the triple-Regge coupling g of Fig. 8(b).

In practice we could assume that the dependence of g on the momentum variables coming into the loop integral of Fig. 8(b) is given by a dual-tree model.^{3,5} Equation (3.11) then determines the overall magnitude of g at each value of t . Appendix D presents an explicit calculation of g at $t = 0$. The result is in reasonable agreement with inclusive cross-section data.

IX. CONCLUSION

We have considered a planar bootstrap model for the hadron spectrum in which simple finite-energy sum rules are combined with infinite sums of ladder graphs. By making a certain simple dynamical approximation we obtain the simple linear form (6.1) for the leading Regge trajectory $\alpha(t)$ in any given equal-mass-channel hadron + hadron \rightarrow hadron + hadron process.

If we impose the requirement that $\alpha(t)$ be independent of the particular process we consider, we obtain powerful self-consistency conditions which we can use to determine the parameters describing the $q\bar{q}$ meson spectrum. These parameters are highly overdetermined in our scheme. The fact that, in spite of this, our conditions are consistent with each other suggests that a more general derivation of Eq. (6.1) than the one presented here probably exists.

We find that we recover most of the usual results of the additive quark model. But we also obtain, without any additional arbitrary parameters, the correct Regge slopes and vector-pseudoscalar mass differences. The latter result is consistent with a quark model in which we add an effective spin-spin term to the long-range interaction (see Appendix A). However, although our results are consistent with such a suitably modified quark model, we can obtain them in terms of a smaller number of *a priori* parameters. Indeed we only have two such parameters, one of which merely fixes the energy scale.

We obtain the usual quark-model result $m_{\eta_s}^2 = 2m_K^2 - m_\pi^2$ for the mass of the η_s , but a higher value $m_{\eta_u}^2 = \frac{1}{2}(m_\rho^2 + 2m_\pi^2)$ for the mass of the η_u . The resulting masses $m_{\eta_s} = 0.687$ GeV and $m_{\eta_u} = 0.462$ GeV are still much lower than the masses of the experimental η' and η . However, cylinder corrections, which go beyond the planar level of our model, are expected to be important in both cases.¹⁹

We actually *derive* an infinitely rising Regge trajectory in our model. If we assume a static interquark interaction this is equivalent to deriving effective confinement. Our model only gives the leading trajectory, which is correlated mainly with the long-range part of this interaction. It might be interesting to study what would happen if we added in a short-range interaction given by one-gluon exchange. This would presumably lead to fine-structure effects for the masses of the particles lying on the lower-lying trajectories. These might be particularly important for the charmonium spectrum, which is currently being investigated.

One of the consequences of the presence of an effective long-range spin-spin interquark interac-

tion in our model is that we no longer have $\alpha_\rho - \alpha_\tau \rightarrow 1$ when $t \rightarrow \infty$, as would be predicted by a quark model which did not have such an interaction. It is sometimes argued that the experimental result $m_{A_2}^2 - m_B^2 < m_\rho^2 - m_\tau^2$ suggests that $\alpha_\rho - 1 \rightarrow \alpha_\tau$ for large t . This argument, however, is based on exact ρ - A_2 and π - B exchange degeneracy. An equally plausible explanation of the mass inequality is to attribute it to the breaking of α_τ - α_B degeneracy due to nonplanar corrections (see, e.g., Chap. 5 of Ref. 10). These corrections would be somewhat larger than the corresponding ones for α_ρ and α_{A_2} , but smaller than the ones for baryon trajectories.

We obtain an η_u which has a different mass from the π in our scheme. This is because the quantum numbers of the η_u are different from those of the π , causing it to couple differently to other particles. Our result contradicts the usual expectation of η_u - π mass degeneracy, which is assumed in most calculations.¹⁹ However, this expectation, while it does not lead to any inconsistencies in most schemes, has never been actually proved from duality in the same general sense that it has for the ω and ρ ; one always has to rely on more specific models. The usual dual-resonance-model proof, for example, assumes an amplitude structure which was abstracted from a class of models which were incapable of incorporating the usual vector trajectories along with the assumed pseudo-scalar trajectories.²⁰

Future calculations using this model might also include:

(i) A study of baryon masses. This would involve a study of baryon-antibaryon scattering, which should give the baryonium spectrum at the same time.¹⁵

(ii) Calculations which do not use assumption (b) of Sec. VI. This assumption is not needed if we take the average of all the clusters consistent with the no-double-counting requirement (1) of Sec. II. Such a calculation requires a knowledge of relative cluster-particle couplings, which would have to be evaluated at the same time—using, perhaps, the methods of Sec. VIII.

(iii) Our simple scheme could be used as a zeroth-order approximation in a more detailed planar-bootstrap calculation. This could, in turn, be used as the input for evaluating higher-order terms in the topological expansion.

ACKNOWLEDGMENTS

The author would like to express his gratitude to Dr. B. Nicolescu for numerous very helpful discussions and correspondences, and to Professor G. F. Chew, Professor S. Mandelstam, Professor K. Gottfried, Dr. Chan Hong Mo, Dr. C. Sorensen,

Dr. Tsou Sheung Tsun, Dr. D. Tow, Dr. M. Bishari, and Professor C. Rosenzweig for valuable comments. This work was supported in part by the U.S. Department of Energy.

APPENDIX A: APPLICATIONS TO $q\bar{q} \rightarrow q\bar{q}$

Strictly speaking, our derivation of Eq. (6.1) is only valid for hadron + hadron \rightarrow hadron + hadron processes. It would be valid for $q\bar{q}$ scattering only if quarks were themselves unconfined physical particles. In this appendix, however, we shall simply *assume* that it continues to apply even when they are confined and have unequal masses. We then find from, say, $u\bar{d}$ scattering that we can generate $\alpha_\rho(t)$ with the parameters of Sec. VI if we take

$$s_a \simeq 2m_u^2, \quad (\text{A1})$$

where m_u is the mass of the u (d) quark. In particular if we take the cluster a to be a massless gluon we see that we must have $m_u^2 \simeq 0$.

Suppose we next include strangeness and assume that the interaction between quarks is flavor independent. This means that the cluster a and output α'_ν must be the same for $u\bar{d}$, $u\bar{s}$, and $s\bar{s}$ scattering. From Eq. (6.1) we then obtain the usual additive-quark-model result

$$t_\phi - t_{K^*} = t_{K^*} - t_\rho = 2(m_s^2 - m_u^2), \quad m_\omega = m_\rho, \quad (\text{A2})$$

which agrees with Eqs. (7.8) and (7.9).

In Sec. V we noted that the quantity L in Eq. (4.14) can be interpreted as an orbital angular momentum. Suppose we then take the usual quark-model prescription that $j = L + 1$ for vector mesons and $j = L$ for pseudoscalar mesons. The latter is equivalent to making the replacement $S_1 + S_2 \rightarrow S_1 + S_2 - 1$ in Eq. (6.1) [see Eq. (4.3)]. If we again assume Eq. (A1), flavor independence immediately gives P - V mass degeneracy with $t_\tau = t_{\eta_u} = t_\rho$, $t_K = t_{K^*}$, and $t_{\eta_s} = t_\phi$.

The simplest way of breaking P - V degeneracy is to drop Eq. (A1) for the pseudoscalar mesons and to take, instead,

$$s_a \simeq 2m_u^2 + \beta(\vec{S}_1 \cdot \vec{S}_2), \quad (\text{A3})$$

where β is a positive constant. This reduces to Eq. (A1) for the vector mesons but gives a higher s_a (and hence lower masses) for the pseudoscalars. With a flavor-independent interaction between the quarks we then have the additive quark-model result

$$t_{\eta_s} - t_K = t_K - t_\tau = 2(m_s^2 - m_u^2), \quad m_{\eta_u} = m_\tau. \quad (\text{A4})$$

From Eqs. (5.3) and (A3) we also see that, if we use the equivalent-potential description of Sec. V, we must have an extra constant $\vec{S}_1 \cdot \vec{S}_2$ term in the

effective long-range interaction. However, unless we consider meson-meson processes, we have no way of calculating β or generating an η_π - π mass difference.

APPENDIX B: CROSSING FOR $\pi\pi$ SCATTERING

Suppose we expand our original "ordered" planar amplitude T in powers of ν for fixed t . Since $T(s, t)$ satisfies a fixed- t dispersion relation

$$T(s, t) = \frac{1}{\pi} \int_0^\infty ds' \frac{A(\nu', t)}{\nu' - \nu}, \quad (\text{B1})$$

where A is the s channel absorptive part, we have

$$T(s, t) = \frac{1}{\pi} [A_0(t) + \nu A_1(t) + \dots], \quad (\text{B2})$$

where A_j is given by Eq. (3.3). If, furthermore, we have, as before, the Regge behavior $A(\nu, t) = b_1 b_2 \nu^\alpha$ for large s , Eq. (3.3) gives

$$A_j(t) = \frac{b_1(t_j) b_2(t_j)}{\alpha'(t_j)(t_j - t)} \quad (\text{B3})$$

near $t = t_j$, where t_j is given by Eq. (8.1). The $A_1(t)$ term in Eq. (B2) then gives

$$T(s, t) = \frac{1}{\pi} \frac{\Gamma(s)}{t_1 - t} \quad (\text{B4})$$

near $t = t_1 = t_\rho$, where

$$\Gamma(s) = \frac{t_\rho - 4m_\pi^2}{2} \frac{b_1(t_\rho) b_2(t_\rho)}{\alpha'(t_\rho)} \left[E + \left(1 + \frac{2s}{t_\rho - 4m_\pi^2} \right) \right]. \quad (\text{B5})$$

We have added an extra positive constant E to take into account any possible $j=0(\epsilon)$ bump at $t \approx t_1$.

Since T is crossing-symmetric,

$$T(s, t) = T(t, s), \quad (\text{B6})$$

and so Eq. (B4) also implies that

$$T(s, t) = \frac{1}{\pi} \frac{\Gamma(t)}{t_\rho - s} \quad (\text{B7})$$

near $s = t_\rho$. From Eq. (B1) this, in turn, corresponds to a contribution to $A(\nu, t)$ given by Eq. (3.5), with $s_a = t_\rho$ and the function Γ given by Eq. (B5). But $\Gamma(t)$ is also given by the finite-energy sum rule (4.5). If we therefore equate Eq. (B5) evaluated at $s = t_\rho$ with Eq. (4.5) evaluated at $t = t_\rho$ we find that we can satisfy crossing at $s = t = t_\rho$ with

$$E = \frac{1}{m_\rho^2 - m_\pi^2} \left[\frac{(3m_\rho^2 - 4m_\pi^2)^2}{8f(m_\rho^2 - m_\pi^2)} + 4m_\rho^2 - 3m_\pi^2 \right]. \quad (\text{B8})$$

Using Eqs. (4.18) and (6.8) this gives $E = 0.54$, which is in fact a small positive number and shows that Γ is dominated by the ρ resonance.

APPENDIX C: $NN \rightarrow \pi\pi$ EXAMPLE

The t -channel $NN \rightarrow \pi\pi$ amplitude can be described in the usual way by the πN amplitude¹⁰

$$T = \bar{u}(q_1) [\mathfrak{A} + \frac{1}{2} \gamma \cdot (q_1 + q_2) \mathfrak{B}] u(q_2), \quad (\text{C1})$$

where \bar{u} , u , and q_1, q_2 are the wave functions and four-momenta of the nucleons involved, and \mathfrak{A} and \mathfrak{B} are the invariant amplitudes. Instead of \mathfrak{A} and \mathfrak{B} it is usually more convenient to deal with \mathfrak{G} and

$$\mathfrak{A}' = \mathfrak{A} + \frac{2M\nu\mathfrak{B}}{1 - t/4M^2}, \quad (\text{C2})$$

where M is the nucleon mass. \mathfrak{B} and \mathfrak{A}' are free of kinematic singularities and satisfy fixed- t dispersion relations. Their s -channel absorptive parts B and A' have the Regge behavior¹⁰

$$B = \eta \nu^{\alpha-1}, \quad (\text{C3})$$

$$A' = \chi \nu^\alpha, \quad (\text{C4})$$

so we have the finite-energy sum rules

$$\int_0^{\bar{s}} ds (B' - \eta \nu^\alpha) \nu^{-1} = 0, \quad (\text{C5})$$

$$\int_0^{\bar{s}} ds (A' - \chi \nu^\alpha) \nu^0 = 0, \quad (\text{C6})$$

where

$$B' = \nu B. \quad (\text{C7})$$

Since $S_1 + S_2 = 1$ for this process, Eq. (C5) corresponds to Eq. (4.1), while Eq. (C6) entails making the replacement $S_1 + S_2 \rightarrow S_1 + S_2 - 1$, as in Eq. (4.3). The amplitudes involved in the two equations are different, although both B' and A' are proportional to ν^α for large s .

APPENDIX D: EXPLICIT TRIPLE-REGGE COUPLING CALCULATION

As discussed in Sec. VIII B, we will assume that $K(j)$ is given by Eq. (3.14). Now for $\pi\pi$ scattering at $t = 0$, with $m_\pi^2 \approx 0$ and $b = c$, Fig. 5(b) gives⁵

$$\begin{aligned} \varphi^2 a^{(2)}(\nu, 0) \approx \frac{1}{16\pi s} \int_{t_-}^{t_+} dt' \gamma_{\pi\pi}^4(t') |X(t')|^2 \\ \times (\alpha' \nu')^{2\alpha(\alpha')} \theta(s - 4s_c), \end{aligned} \quad (\text{D1})$$

where

$$X(t) = e^{-i\pi\alpha(\alpha')/\sin\pi\alpha(t)}, \quad (\text{D2})$$

$$t_\pm \approx -\frac{1}{4} [s^{1/2} \mp (s - 4s_c)^{1/2}]^2, \quad (\text{D3})$$

$$\nu' \approx s + \frac{1}{2}(t' - 2s_c). \quad (\text{D4})$$

To simplify our problem further we will assume

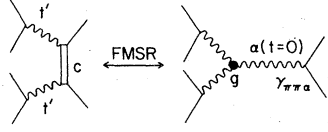


FIG. 12. Finite-mass sum rule FMSR for $\pi\pi \rightarrow \pi X$ relating cluster production and triple-Regge regions.

that we can replace t_{\pm} by their asymptotic forms for $s > 4s_c$. Equation (D1) then reduces to

$$\varphi^2 a^{(2)}(\nu, 0) \simeq \frac{1}{16\pi s} \int_{-\infty}^0 dt' \gamma_{\pi c \alpha}^4(t') |X(t')|^2 \times (\alpha' \nu')^{2\alpha(t')} \theta(s - 4s_c). \quad (\text{D5})$$

If we take the Mellin transform (3.3) of Eq. (D4) we obtain

$$\varphi^2 a_j^{(2)}(0) = \frac{\alpha'^{j+1}}{16\pi} \int_{-\infty}^0 \frac{dt'}{j+1-2\alpha(t')} \gamma_{\pi c \alpha}^4(t') |X(t')|^2 \times [\alpha'(3s_c + \frac{1}{2}t')]^{2\alpha(t')-j-1}. \quad (\text{D6})$$

To relate the dimensionless coupling $\gamma_{\pi c \alpha}$ to a triple-Regge coupling we will use the usual finite-mass sum rule (FMSR) for the inclusive process $\pi\pi \rightarrow \pi X$ in the limit $s \rightarrow \infty$,

$$\int_0^{\bar{M}_0^2} d\bar{M}^2 \left[\frac{d\sigma}{dt' dM^2} - \frac{G(t')}{s^2} \left(\frac{s}{\bar{M}^2} \right)^{2\alpha(t')} (\alpha' \bar{M}^2)^{\alpha(0)} \right] = 0, \quad (\text{D7})$$

where

$$G(t') = \frac{\alpha'}{16\pi} \gamma_{\pi\pi\alpha}^2(t') |X(t')|^2 g(t', t', 0) \gamma_{\pi\pi\alpha}(0), \quad (\text{D8})$$

$\bar{M}^2 = M^2 - t' - m_\pi^2$, M is the missing mass, and g is the dimensionless $\alpha\alpha\alpha$ triple-Regge coupling (see Fig. 12). We will assume that the low- M^2 region is dominated by c production, so that, in the narrow-resonance approximation

$$\frac{d\sigma}{dt' dM^2} = \left(\frac{d\sigma}{dt'} \right)_c \delta(M^2 - s_c), \quad (\text{D9})$$

where $(d\sigma/dt')_c$ is the usual differential cross section for $\pi\pi \rightarrow \pi c$, which is given by

$$\left(\frac{d\sigma}{dt'} \right)_c = \frac{1}{16\pi s^2} \gamma_{\pi\pi\alpha}^2(t') |X(t')|^2 \times \gamma_{\pi c \alpha}^2(t') (\alpha' s)^{2\alpha(t')}. \quad (\text{D10})$$

Since the spacing between resonances lying on $\alpha(t)$ is α'^{-1} , we will take the separation point M_0^2 to be

$$M_0^2 \simeq s_c + \frac{1}{2} \alpha'^{-1}. \quad (\text{D11})$$

From Eqs. (D6)–(D9) we then have

$$\gamma_{\pi c \alpha}^2(t') = \frac{g(t', t', 0) \gamma_{\pi\pi\alpha}(0)}{\alpha(0) + 1 - 2\alpha(t')} \times (\alpha' \bar{M}_0^2)^{\alpha(0)+1-2\alpha(t')}. \quad (\text{D12})$$

If we now combine Eqs. (3.11), (3.14), (3.6), (4.5), (D6), and (D12) at $t=0$, and use the fact that $b_1 b_2 = \gamma_{\pi\pi\alpha}^2 \alpha'^{\alpha(0)}$, we obtain the condition

$$\frac{\alpha(0) + 1}{16\pi f} \int_{-\infty}^0 dt' \frac{H(t')}{\alpha(0) + 1 - 2\alpha(t')} = \frac{1}{\alpha'}, \quad (\text{D13})$$

where

$$H(t') = \frac{g^2(t', t', 0) |X(t')|^2}{[\alpha(0) + 1 - 2\alpha(t')]^2} \times \left(\frac{\alpha' \bar{M}_0^4}{3s_c + \frac{1}{2}t'} \right)^{\alpha(0)+1-2\alpha(t')}.$$

We will assume that g is given by a dual-tree model of the Neveu-Schwartz type, which has no tachyon on the ρ - f trajectory. This gives

$$g^2(t, t, 0) |X(t)|^2 = N \bar{g}^2 \Gamma(\alpha(0)) \frac{\Gamma^2(1 - \alpha(t))}{\Gamma^2(\alpha(0) + 1 - 2\alpha(t))}, \quad (\text{D14})$$

where N is the number of quarks and \bar{g} is a reduced coupling.

Equation (D13) involves a nonelementary integral. However, the integrand falls off fairly rapidly with t' and so we will approximate $H(t')$ by an exponential

$$H(t') \simeq H(0) e^{2ct'} \quad (\text{D15})$$

with c adjusted so that $H'(0)$ is exact. Equation (D13) then reduces to

$$\frac{H(0)}{16\pi} \exp \left\{ [1 - \alpha(0)] \frac{c}{\alpha'} \right\} E_1 \left([1 - \alpha(0)] \frac{c}{\alpha'} \right) = \frac{f}{\alpha(0) + 1}, \quad (\text{D16})$$

where E_1 is the usual exponential integral. If we take s_0 to be the natural threshold of Fig. 5(c), we have $s_0 = 4s_c$. From Eq. (6.9) we then have $s_c \simeq \frac{1}{2} m_\rho^2$. With the trajectory parameters given by Eq. (6.8) and f given by Eq. (4.18), Eq. (D16) then gives

$$N \bar{g}^2 / 16\pi \simeq 0.94. \quad (\text{D17})$$

This is quite close to the value extracted from experiment in Refs. 5 and 11.

APPENDIX E: UNEQUAL-MASS-CHANNEL PROCESSES

We have argued in Sec. III that our approach may not be reliable when $m_1 \neq m_2$ or $m_3 \neq m_4$. In this appendix, however, we shall investigate

whether Eq. (6.1) continues to apply for such processes anyway, given the results derived from equal-mass-channel processes.

For simplicity we shall restrict ourselves to the simple case considered in Sec. VI with degenerate V and P multiplets. In addition to Eqs. (6.11)–(6.13) we can now have the following processes generating α_V :

$$\alpha_P \alpha_V(a_5) P V \rightarrow \alpha_V, \quad (\text{E1})$$

$$\alpha_P \alpha_V(a_6) V P \rightarrow \alpha_V, \quad (\text{E2})$$

$$\alpha_V \alpha_V(a_7) V P \rightarrow \alpha_V, \quad (\text{E3})$$

$$\alpha_P \alpha_V(a_8) P P \rightarrow \alpha_V. \quad (\text{E4})$$

These processes are consistent with Eq. (6.1) and the results of Sec. VI provided we take

$$s_{a_5} = s_{a_6} = m_V^2, \quad (\text{E5})$$

$$s_{a_7} = s_{a_8} = m_P^2 + \frac{1}{2}(m_V^2 - m_P^2). \quad (\text{E6})$$

But G parity would exclude any P contributions to a_8 in Eq. (E4). This means that we must have $s_{a_8} \geq m_V^2$, which contradicts Eq. (E6), since $m_P < m_V$. We conclude that either Eq. (6.1) simply does not apply to Eq. (E4) or the coupling V - P - α_V must vanish at the level of approximation being considered here; it may of course be nonzero when we include higher-order corrections.

With V - P - $\alpha_V = 0$, Eqs. (E1)–(E4) drop out and the only processes we are left with are Eq. (6.11)–(6.13). In the case of processes generating α_P , Eq. (6.16) also drops out, but we can now have

$$\alpha_P \alpha_V(a_9) V P \rightarrow \alpha_P, \quad (\text{E7})$$

where the cluster a_9 must contain P and, perhaps, its $j=1$ Regge recurrence P^r . The process (E7) is consistent with Eq. (6.1) provided we take

$$s_{a_9} = \frac{1}{4}(3m_P^2 + m_{P^r}^2). \quad (\text{E8})$$

¹J. L. Rosner, Phys. Rep. **11C**, 189 (1974).

²G. F. Chew and C. Rosenzweig, Phys. Rep. **41C**, 263 (1978).

³C. Rosenzweig and G. Veneziano, Phys. Lett. **52B**, 335 (1974).

⁴M. Schaap and G. Veneziano, Lett. Nuovo Cimento **12**, 204 (1975); K. Konishi, Nucl. Phys. **B116**, 356 (1976); J. Millan (unpublished).

⁵L. A. P. Balázs, Phys. Rev. D **15**, 319.

⁶A. De Rújula, H. Georgi, and S. L. Glashow, Phys. Rev. D **12**, 147 (1975).

⁷T. A. De Grand, R. L. Jaffe, K. Johnson, and J. Kiskis, Phys. Rev. D **12**, 2060 (1975).

⁸G. Veneziano, in *Color Symmetry and Quark Confinement*, proceedings of the XII Rencontre de Moriond, Flaine, 1977, edited by J. Trân Thanh Vân (Editions Frontières, Paris, 1977).

⁹G. Veneziano, Nucl. Phys. **B74**, 365 (1974); Phys. Lett.

52B, 220 (1974).

¹⁰P. D. B. Collins, *An Introduction to Theory and High Energy Physics* (Cambridge University Press, Cambridge, England, 1977).

¹¹Chan Hong-Mo, J. E. Paton, and Tsou Sheung Tsun, Nucl. Phys. **B86**, 479 (1975).

¹²L. A. P. Balázs, Phys. Rev. D **16**, 885 (1972).

¹³L. A. P. Balázs, Phys. Rev. D **2**, 999 (1970) (Appendix C); Phys. Lett. **29B**, 228 (1969).

¹⁴L. A. P. Balázs, Phys. Lett. **71B**, 216 (1977).

¹⁵L. A. P. Balázs and B. Nicolescu, Phys. Lett. **72B**, 240 (1977).

¹⁶L. A. P. Balázs, Lett. Nuovo Cimento **23**, 56 (1978).

¹⁷C. Lovelace, Phys. Lett. **28B**, 264 (1968).

¹⁸L. A. P. Balázs, Phys. Rev. D **17**, 3124 (1978).

¹⁹J. Millan, Phys. Rev. D **15**, 2695 (1977).

²⁰P. H. Frampton, *Dual Resonance Models* (Benjamin, Reading, Mass., 1974).